

Tetrahydrofuran in $\text{TiCl}_4/\text{THF}/\text{MgCl}_2$: a Non-Innocent Ligand for Supported Ziegler–Natta Polymerization Catalysts

Etienne Grau,^{†,‡,§} Anne Lesage,^{||} Sébastien Norsic,[‡] Christophe Copéret,^{*,†} Vincent Monteil,^{*,‡} and Philippe Sautet^{*,§}

[†]Department of Chemistry, ETH Zurich, Wolfgang-Pauli-Strasse 10, 8093 Zurich, Switzerland

[‡]Université de Lyon, Univ. Lyon 1, CPE Lyon, CNRS, Chimie Catalyse Polymères et Procédés (C2P2), LCPP team, 43 Bd du 11 novembre 1918, 69616 Villeurbanne, France

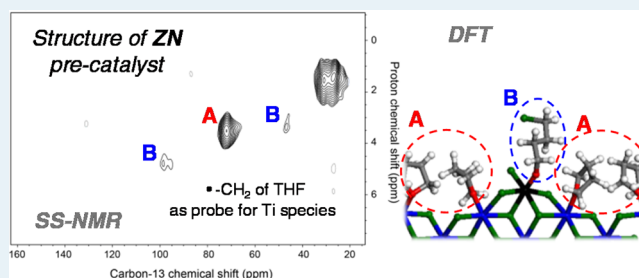
[§]Université de Lyon, CNRS, Ecole Normale Supérieure de Lyon, Laboratoire de Chimie, 46 Allée d'Italie, 69364 Lyon Cedex 07, France

^{||}Université de Lyon, CNRS, Ecole Normale Supérieure de Lyon, Centre de RMN à Très Hauts Champs, 5 rue de la Doua, 69100 Villeurbanne, France

Supporting Information

ABSTRACT: While Ziegler–Natta (ZN) polymerization is one of the most important catalytic industrial processes, the atomic-scale nature of the catalytically active surface species remains unknown. Coupling high-resolution solid-state NMR spectroscopy with periodic density functional theory (DFT) calculations, we demonstrate that the major surface species in the ZN pre-catalyst corresponds to an alkoxy Ti(IV) surface species, which probably results from the ring-opening of tetrahydrofuran (THF) on a cationic Ti(IV) species.

KEYWORDS: ethylene polymerization, Ziegler–Natta catalysis, surface chemistry, SS-NMR spectroscopy, DFT calculations



The current generation of heterogeneous catalytic systems for the production of polyolefins, based on titanium chloride supported on magnesium dichloride referred to as Ziegler–Natta (ZN) catalyst, is one of the most advanced industrial applications of catalysis.^{1–5} Despite major research efforts for the understanding of the organization of the active sites of these complex catalysts, in particular by addressing structure activity/selectivity relationships, the structure of the active sites has remained elusive.^{1–5} While it is clear that the MgCl_2 -based support is here not merely to disperse the active Ti phase, its specific role as well as the structure of surface Ti species, even prior to activation with alkylaluminum compounds, remain largely unknown at the molecular level despite years of research combining experimental^{6–12} and theoretical investigations.^{13–22}

In fact, one of the key steps in generating highly active ZN catalysts is the preparation method of the pre-catalyst prior to its activation by an alkylaluminum compound (referred to as cocatalyst), which finally triggers the polymerization of olefins. It concerns the preparation of MgCl_2 and its subsequent contact with titanium complexes such as TiCl_4 . Both, mechanical and chemical routes are used to obtain “active” MgCl_2 -supported titanium ZN pre-catalyst.^{2,3} The latter may involve the reaction of solid MgCl_2 with a Lewis base, typically an alcohol^{23–26} such as ethanol or an ether^{27–30} such as tetrahydrofuran (THF). This step is usually followed by a treatment with a large excess of TiCl_4 providing then highly

active catalysts. The use of THF in pre-catalyst synthesis is an important industrial route to prepare catalysts for the production of polyethylene.

Here by combining high-resolution solid-state NMR spectroscopy and Density Functional Theory (DFT) periodic calculations, we unravel the atomic structure of Ti surface species in a highly active pre-catalyst, $\text{MgCl}_2/\text{THF}/\text{TiCl}_4$, involved in ZN polymerization of ethylene. We clearly evidence that the nature of Ti species is modified by the interaction with MgCl_2 and THF to give a transient cationic Ti mononuclear species, which finally leads to a neutral alkoxy Ti species via the ring-opening of THF. Beyond its important role as a promoter of MgCl_2 , THF is used here as an in situ probe to reveal the structure of the Ti surface species, the chemical shift of the α -carbons providing a very sensitive spectroscopic signature. The formation of such alkoxy Ti species was also found for ZN pre-catalysts based on MgCl_2 -alcohol supports.

The ZN pre-catalyst used in this study was prepared as follows: MgCl_2 was stirred in boiling THF during 4 h. A white solid corresponding to $\text{MgCl}_2(\text{THF})_x$ with $x \approx 1.5$ was isolated by decantation and successive washing with heptane. This solid was then contacted with an excess of pure TiCl_4 at 90 °C during 2 h. After decantation, the solid was washed with hot

Received: November 27, 2012

Published: December 4, 2012

toluene and then heptane yielding a yellow powder, named ZN precatalyst in the following. The ZN precatalyst was characterized in detail as follows. The solid contains 3%wt of Ti, 16%wt of Mg, and 27%wt of THF, thus giving the $\text{MgCl}_2(\text{THF})_{0.57}(\text{TiCl}_4)_{0.09}$ average molecular formula and a ratio THF/Ti close to 6. The X-ray powder diffraction pattern is typical of layered $\alpha\text{-MgCl}_2$ with extensive structural disorder (Supporting Information, Figure S1). It is noteworthy to mention that the ZN precatalyst displays no Electron Paramagnetic Resonance (EPR) signal and can be characterized by NMR (vide infra) consistent with the absence of isolated Ti(III) in the precatalyst. The ZN precatalyst provides a highly active catalyst for polymerization of ethylene after activation by triethylaluminum (TEA): an activity of $5000 \text{ gPE}\cdot\text{gcat}^{-1} \text{ h}^{-1}$ was measured under standard conditions (7 bar of ethylene and 1 bar of H_2 at 80°C). Polyethylene produced exhibits expected properties ($M_n = 60000 \text{ g/mol}$, $D = 4.6$ and a melting temperature of 135.5°C).

To gain insight into the molecular structure of surface species, the ZN precatalyst was further analyzed by magic angle spinning (MAS) solid-state NMR spectroscopy. Both, two-dimensional (2D) $^1\text{H}\text{-}^{13}\text{C}$ heteronuclear correlation (HETCOR) (Figure 1) and 2D proton double-quantum (DQ)

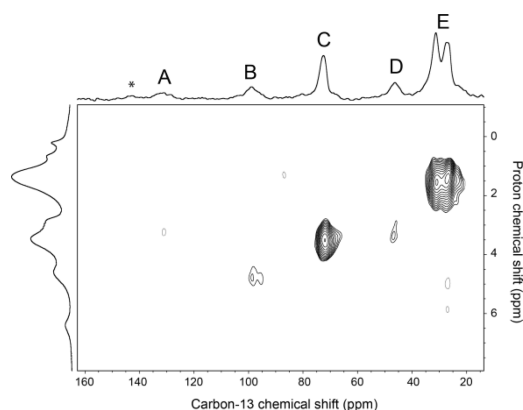


Figure 1. 2D $^1\text{H}\text{-}^{13}\text{C}$ HETCOR solid-state NMR spectrum of $\text{MgCl}_2/\text{TiCl}_4/\text{THF}$ ZN precatalyst. The 1D ^1H and ^{13}C CPMAS spectra are displayed respectively on the left and on the top of the 2D map. These spectra were recorded at 800 MHz (proton frequency) using a spinning frequency of 22 kHz. Other experimental details are given in the Supporting Information.

single-quantum (SQ) correlation spectroscopy (Supporting Information, Figure S2) were applied. The one-dimensional (1D) carbon-13 cross-polarization (CP) spectrum displays 6 main peaks: 132, 97, 72, 46, 31, and 25 ppm (Figure 1, top). Signals at 72 ppm on one hand (C) and at 31 and 25 ppm (E) on the other hand can be readily assigned to respectively to the α - and β -carbons of THF molecules coordinated on the ZN precatalyst. Two well-separated peaks are observed for the α -carbons, indicating distinct environments for these THF molecules. The signal at 132 ppm (A) corresponds to the aromatic ring carbons of adsorbed toluene, used during the washing steps (as expected the addition of toluene on the precatalyst increases the intensity of this peak; Supporting Information, Figure S3). The resonance of the methyl carbons, expected at about 21 ppm, is likely masked by the signal of the β -carbons of THF. The two other signals at 97 (B) and 46 (D) ppm are unexpected as they are strongly shifted with respect to

the resonances of coordinated THF and cannot be readily interpreted.

The 2D $^1\text{H}\text{-}^{13}\text{C}$ HETCOR spectrum (Figure 1) displays four main correlation peaks at $[(\delta\text{-}^1\text{H}) \text{ ppm}/(\delta\text{-}^{13}\text{C}) \text{ ppm}]$: [4.7/97], [3.5/72], [3/46], and [1.5/28]. Resonances C and E correlate with protons at around respectively 3.5 and 1.5 ppm respectively, which is in good agreements with the α and β ^1H chemical shifts expected for THF molecules coordinated on the ZN precatalyst. A HETCOR spectrum recorded with a longer CP contact time (Supporting Information, Figure S4) shows the expected long-range correlations between the α and β resonances of the coordinated THF. Two clear correlations are also observed for peaks B and D with protons at around respectively 4.7 and 3 ppm. These two proton resonances can be unambiguously assigned to THF α protons from a 2D ^1H DQ-SQ correlation spectrum recorded at 60 kHz MAS (Supporting Information, Figure S2, a). Indeed clear correlations are observed at $(\omega_{\text{DQ}}/\omega_{\text{SQ}}) = (6.3/4.7)$ and $(6.3/1.6)$ ppm on the one hand and at $(\omega_{\text{DQ}}/\omega_{\text{SQ}}) = (4.6/1.6)$ ppm on the other hand, that is, correlations between these proton resonances at 4.7 and 3 ppm and the intense peak at 1.6 ppm corresponding to the β protons of THF. Thus, on the carbon-13 spectrum, while resonance C corresponds to the α -carbons of adsorbed THF molecules, peaks B and D are attributed to α -carbons of additional, unexpected, surface species. Note, that, as expected, strong correlations are also observed in the 2D ^1H DQ-SQ spectrum between the α and β protons of the THF molecules adsorbed on the precatalyst at (4.9/3.5) and (4.9/1.4) ppm, as well as weak cross-peaks at (8.1/6.4) and (8.1/1.7) ppm between the two proton resonances of adsorbed toluene (Supporting Information, Figure S2, b). In addition, all proton resonances display strong autocorrelation peaks as they all correspond to CH_2 groups. Purely based on chemical shifts, B is reminiscent of the α -carbon of THF coordinated to a cationic Ti center,^{31,32} while D would be in line with a methylene carbon in α of a chlorine atom; one possibility would be that this results from the presence of a 4-chloro-butan-1-oxy derivatives originating from the potential ring-opening of THF upon interaction of TiCl_4 with $\text{MgCl}_2\text{-THF}$.

To confirm this hypothesis and determine the exact nature of the Ti surface complexes, we explored via periodic DFT calculations the stability of species resulting from the interactions between THF and TiCl_4 on MgCl_2 and calculated the NMR signatures of the corresponding surface species.

Numerous surface species can be present on the precatalyst (Figure 2): THF coordinated to Mg (0), THF coordinated to Mg close to Ti (I), THF coordinated to cationic Ti^+ (II) or

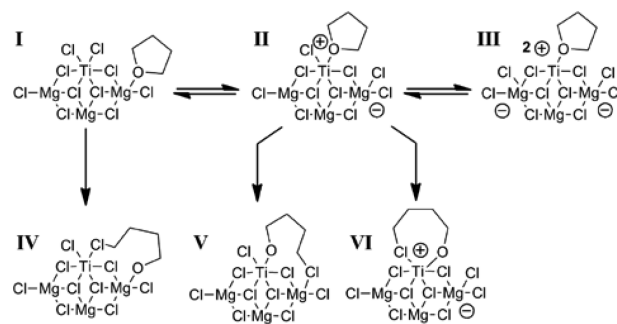


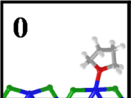
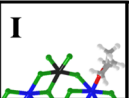
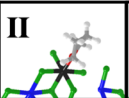
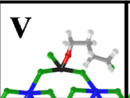
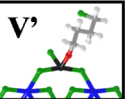
Figure 2. Schematic structure for the Ti surface species and possible mechanisms for THF opening.

even THF coordinated to dicationic Ti^{2+} (**III**) as well as 4-chloro-butan-1-ol coordinated to Mg (**IV**), Ti (**V**) or Ti^+ (**VI**).

The structures of such species were investigated by adsorbing THF and/or TiCl_4 on periodic models of the (001), (104), and (110) surfaces of $\alpha\text{-MgCl}_2$, and the corresponding NMR chemical shifts were then calculated using $(\text{MgCl}_2)_{10}$ clusters. MgCl_2 bulk and surfaces were calculated (Supporting Information, Figure S5 and Table S1) with the PW91 GGA exchange-correlation functional together with the Grimme method to describe van der Waals interactions between MgCl_2 layers, using the VASP implementation.^{33–35} A cutoff energy of 400 eV for the plane-wave basis set provided converged energies. Coordination of THF and TiCl_4 was investigated on the (104) and (110) surfaces (Supporting Information, Figure S6). In agreement with previous studies,^{19,22} a much more favorable adsorption was found on the (110) surface of $\alpha\text{-MgCl}_2$. As a consequence, this surface was used for further study of the coadsorption of THF and TiCl_4 . In all surface calculations, a (3×1) supercell containing 9 surface Mg, a 10 layer thick MgCl_2 slab with the first 5 being relaxed, and a vacuum of 10 Å between slabs were used (Supporting Information, Figure S7). In a second step a $(\text{MgCl}_2)_{10}$ cluster was extracted to perform calculations of nuclear magnetic shielding tensors using Gaussian09 with the B3PW91 hybrid functional and a high quality 6-311++G(d) basis set.³⁶

In Table 1 are summarized the relative energies and the ^{13}C NMR chemical shifts changes with respect to free THF

Table 1. Calculated Co-Adsorption Energies for Different THF and TiCl_4 Species on MgCl_2 (110), Differential Adsorption Energies ($\Delta\Delta E$) and ^{13}C NMR Chemical Shifts versus Free THF^a

	0	I	II	V	V'
					
E_{ads} (kJ mol ⁻¹)	∞	-334	-345	-269	-306
$\Delta\Delta E$ (kJ mol ⁻¹)	11	0 (ref)	76	39	63
^{13}C NMR shift vs free THF (ppm)		$\alpha\text{-O: } +1.0$ $\beta\text{-O: } -1.2$	$\alpha\text{-O: } +2.6$ $\beta\text{-O: } +1.7$	$\alpha\text{-O: } +22.5$ $\beta\text{-O: } +2.5$ $\alpha\text{-Cl: } -13.6$ $\beta\text{-O: } +3.4$ $\beta\text{-Cl: } +2.9$	$\alpha\text{-O: } +24.3$ $\alpha\text{-Cl: } -19.2$ $\beta\text{-O: } +6.1$ $\beta\text{-Cl: } +5.9$

^aFor ^1H NMR see Supporting Information, Table S2. The energy references are THF in $\text{TiCl}_4(\text{THF})_2$ and TiCl_4 in gas phase for THF and TiCl_4 respectively. Color chart: in blue Mg atom, green Cl, black Ti, red O, gray C, pale gray H.

molecules for the different THF and TiCl_4 coadsorption species on the MgCl_2 (110) surface. THF prefers (with a gain of 11 kJ mol⁻¹) to be coordinated to a Mg adjacent to a neutral Ti site (**I**) than far from it, indicating that the Lewis acidity of Mg is enhanced by the Ti center.^{37,38} In both cases the ^{13}C and ^1H chemical shifts are mostly unchanged. These data are thus

consistent with the assignment of resonances **C** and **E** correlation to THF coordinated to Mg whether close or far from a Ti center.

The coordination of THF to Ti and the transfer of one of the Cl ligand to an adjacent Mg yield a formally cationic Ti^+ species (**II**), which corresponds to an “ate” complex. This ligand permutation from **I** to **II** is endoenergetic by 76 kJ mol⁻¹. From the strong Lewis acidity of the Ti^+ cation, THF in this species displays significant downfield shifts for the α -nuclei compared to free THF or THF on Mg: namely +20 ppm and +1.5 ppm for $\alpha\text{-C}$ and $\alpha\text{-H}$, respectively, while the β -nuclei are barely affected. Such shifts would be consistent with the observed correlation peak at (4.6/97) ppm in the HETCOR spectrum (corresponding to peak **B**). The displacement of a second Cl ligand leads to the formation of an unstable dicationic Ti species (**III**); in fact ionic relaxation brings the system back to the monocationic species (**II**). However **III** can be found as a metastable minimum when two THF are coordinated on Ti giving NMR chemical shifts similar to **II** (Supporting Information, Figure S8 and Tables S2–S3).

So far, none of the calculated species allows the interpretation of the carbon-13 upfield shift observed experimentally for peak **D** (−25 ppm). In addition cationic species are much less stable than the neutral species such as **I** (Supporting Information, Figure S8). In view of the possible formation of 4-chloro-butan-1-ol species by the ring-opening of THF, we therefore investigated the corresponding species as depicted in Figure 2 and Supporting Information, Figure S8. This process is thermodynamically favored only from **II** to **V** (−37 kJ mol⁻¹) while the formation of **IV** (+192 kJ mol⁻¹) or **VI** (+147 kJ mol⁻¹) are highly endoenergetic (Supporting Information, Table S3). Note that structures slightly less stable than **V**, where the chlorine atom of the 4-chlorobutoxy ligand is not coordinated to an adjacent Lewis acid site (Mg) (**V'**) or coordinated to a sublayer Mg atom (**V''**), can also be proposed.

All these surface complexes are associated with significant NMR chemical shift changes with respect to the reference structure **I** (Supporting Information, Table S2): (i) **IV** induces downfield shifts of approximately 10 ppm for both α - and β -carbons; (ii) **V** displays shifts of +21.4 ppm and −13.6 ppm for the carbons in α of oxygen and chlorine, respectively; (iii) **VI** and **V'** have chemical shifts similar to **V**. Of all structures, **V'** is the only species whose associated calculated chemical shifts are consistent with the remaining unassigned correlation peak at (3/46) ppm in the HETCOR spectrum (and corresponding to peak **D** in the 1D ^{13}C spectrum). More specifically, the ^{13}C calculated shifts with respect to free THF molecules are −19.2 ppm for the carbon in α of chlorine, +24.3 ppm for the one in α of oxygen, +5.9 and +6.1 ppm for the β carbons. These chemical shifts are in good agreement with those observed experimentally for resonances **B**, **D**, and **E** respectively. It is noteworthy to mention that the release of the chlorine atom of **V** to form **V'** is endoenergetic by +24 kJ mol⁻¹. The entropic term favors however the pendant chlorine in **V'** (Supporting Information, Figure S9).

The combination of high-resolution solid-state NMR and periodic calculations thus points out the formation of Ti 4-chlorobutoxy species (especially **V'**) at the surface of $\text{MgCl}_2/\text{THF}/\text{TiCl}_4$ precatalyst. To obtain even more direct evidence of the presence of these alkoxy species, a precatalyst was prepared by replacing THF by 4-chlorobutan-1-ol (ClBuOH). This $\text{MgCl}_2/\text{ClBuOH}/\text{TiCl}_4$ precatalyst was obtained by contacting with an excess of pure TiCl_4 the corresponding solid support

$\text{MgCl}_2(\text{ClBuOH})_x$ with $x \approx 1$ using the same receipt described for $\text{MgCl}_2/\text{THF}/\text{TiCl}_4$ precatalyst, and it displayed similar activities ($1200 \text{ gPE-gcat}^{-1}\text{h}^{-1}$). The 1D carbon-13 CP spectrum of $\text{MgCl}_2/\text{ClBuOH}/\text{TiCl}_4$ precatalyst displays four main peaks at 96, 48, 45, and 29 ppm while the corresponding support shows three peaks at 63, 45, and 29 ppm (Supporting Information, Figure S10). For the support, the peaks are easily assigned to methylene carbons in α to oxygen (63 ppm), in α to chlorine (45 ppm), and to the methylene carbons in β (29 ppm) of 4-chlorobutan-1-ol adsorbed at the MgCl_2 surface. The spectrum of the precatalyst clearly demonstrates the formation of Ti 4-chlorobutoxy species as evidenced by the shift of the methylene carbon in α to oxygen from 63 to 96 ppm. The β methylene carbons chemical shifts remain unchanged at 29 ppm while the peak corresponding to the CH_2 in α to chlorine is split into two signals at 45 and 48 ppm (probably depending whether the chlorine atom interact with Ti or not at the precatalyst surface). The comparison with the spectrum of $\text{MgCl}_2/\text{THF}/\text{TiCl}_4$ precatalyst further confirms that the resonances **B** and **D** at 97 and 46 ppm, respectively, can be assigned to Ti 4-chlorobutoxy species (**V'**). In fact, alcoholysis of both precatalysts yield 1,4-dichlorobutane and traces of 4-chlorobutanol; the former resulted from the acid-catalyzed nucleophilic substitution of the OH by Cl. This also applies to ethanol-based ZN catalysts,^{23–26} where ethoxy species are observed (Supporting Information, Figure S11), making the presence of alkoxy surface species very general.

While the calculated chemical shifts for species **0**, **I**, and **V'** match very well the observed shifts and fully explain the observed NMR spectra, the relative energy for **V'** compared to **I** would predict that **V'** should be only very minor species. Since the experimental system corresponds to a large coverage of THF per surface Ti, we finally explored the effect of additional THF molecules on the relative stability of the various species. Calculations with two to five THF per row of the surface cell (i.e., for 3 surface Mg and one Ti) were thus performed (Supporting Information, Figure S8, S12 and Table S3). It should be noted that increasing the THF coverage does not affect the calculated chemical shifts (Supporting Information, Table S2). Interestingly **V'** corresponding to the species with opened THF and a pendant Cl is stabilized versus other species by additional THF making it more stable than **V** at high THF content and slightly more stable than **I** (Supporting Information, Figure S12). In view of the experimental conditions (large excess of THF), the comparison of experimental and calculated NMR signatures and the relative energies of possible structures, it is clear that **V'**, a neutral Ti alkoxy species resulting from the ring-opening of THF on a cationic Ti center, is a surface species present in $\text{MgCl}_2/\text{THF}/\text{TiCl}_4$ precatalyst. This structure fully explains the ^{13}C resonances labeled **B**, **D**, and **E**. Moreover, this **V'** species is favored by the presence of adjacent THF which correspond in large part to resonances **C** and **E**.

In view of the empirical formula for the precatalyst— $\text{MgCl}_2(\text{THF})_{0.57}(\text{TiCl}_4)_{0.09}$ (6 THF per total Ti)—and the presence of NMR signals corresponding to two distinct surface species in a about 5-to-1 ratio, the former associated with coordinated THF and the latter with ring-opened THF, and the relative stability of surface species based on computational calculations, the data are consistent with the formation of a majority of Ti alkoxy species (**V'**) surrounded by at least 4 THF coordinated on adjacent Mg sites.

In conclusion, the combination of solid-state NMR spectroscopy and periodic calculations has been essential to provide a molecular understanding of the nature of the surface species in $\text{MgCl}_2/\text{THF}/\text{TiCl}_4$ ZN precatalyst. In particular, this study points out that the major surface sites are Ti alkoxy surface species, that result from the opening of THF via cationic Ti/THF transient intermediate, and surrounded by THF coordinated to nearby Mg. Such Ti alkoxy surface species are also present at the surface of alcohol based precatalysts. Hence THF (or equivalently alcohol) is not merely a solvent, but actively takes part in the creation of the surface active sites. In view of the difference of reactivity of alkoxy vs chloro titanium compounds toward alkyl aluminum compounds, we are currently investigating how this key Ti alkoxy species impacts the formation and the nature of the active species for the chain-growth in ZN catalysis upon activation.

■ ASSOCIATED CONTENT

☛ Supporting Information

Text giving experimental details, figures showing X-rays scattering of precatalyst, NMR data of various catalysts, orthogonal view of different MgCl_2 surface and their energies, orthogonal view of adsorbed THF and TiCl_4 on these surfaces, zoom on different $\text{TiCl}_4(\text{THF})_{1-5}$ species on (110) surface and their relative energies and calculated NMR shifts. This material is available free of charge via the Internet at <http://pubs.acs.org>.

■ AUTHOR INFORMATION

Corresponding Author

*E-mail: ccoperet@inorg.chem.ethz.ch (C.C.), monteil@lcpp.cpe.fr (V.M.), philippe.sautet@ens-lyon.fr (P.S.).

Notes

The authors declare no competing financial interest.

■ ACKNOWLEDGMENTS

The authors want to thank Roger Spitz for his fruitful contribution to Ziegler–Natta catalysis over the years. Financial support from the TGE RMN THC Fr3050 for conducting the research is gratefully acknowledged. Finally, the authors thank the PSMN at ENS Lyon where calculations were done.

■ REFERENCES

- (1) Pino, P.; Mülhaupt, R. *Angew. Chem., Int. Ed. Engl.* **1980**, *19*, 857–875.
- (2) Barbé, P. C.; Cecchin, G.; Noristi, L. *Adv. Polym. Sci.* **1987**, *81*, 1–77.
- (3) Albizzati, E.; Giannini, U.; Collina, G.; Noristi, L.; Resconi, L. Catalyst and Polymerizations. In *Polypropylene Handbook*; Moore, E. P., Ed.; Hanser-Gardner Publications: Cincinnati, OH, 1996; Chapter 2.
- (4) Mülhaupt, R. *Macromol. Chem. Phys.* **2003**, *204*, 289–327.
- (5) Eisch, J. J. *Organometallics* **2012**, *31*, 4917–4932.
- (6) Magni, E.; Somorjai, G. A. *Surf. Sci.* **1996**, *345*, 1–16.
- (7) Mori, H.; Sawada, M.; Higuchi, T.; Hasebe, K.; Otsuka, N.; Terano, M. *Macromol. Rapid Commun.* **1999**, *20*, 245–250.
- (8) Fregonese, D.; Glisenti, A.; Mortara, S.; Rizzi, G. A.; Tondello, E.; Bresadola, S. *J. Mol. Catal. A: Chem.* **2002**, *178*, 115–123.
- (9) Schmidt, J.; Risse, T.; Hamann, H.; Freund, H.-J. *J. Chem. Phys.* **2002**, *116*, 10861–10868.
- (10) Kim, S. H.; Somorjai, G. A. *Proc. Natl. Acad. Sci.* **2006**, *103*, 15289–15294.
- (11) Andoni, A.; Chadwick, J. C.; Niemantsverdriet, H. J. W.; Thüne, P. C. *Macromol. Rapid Commun.* **2007**, *28*, 1466–1471.

- (12) Groppo, E.; Seenivasan, K.; Barzan, C. *Catal. Sci. Technol.* **2013**, Advance Article, DOI: 10.1039/C2CY20559A.
- (13) Boero, M.; Parrinello, M.; Terakura, K. *J. Am. Chem. Soc.* **1998**, *120*, 2746–2752.
- (14) Cavallo, L.; Guerra, G.; Corradini, P. *J. Am. Chem. Soc.* **1998**, *120*, 2428–2436.
- (15) Toto, M.; Morini, G.; Guerra, G.; Corradini, P.; Cavallo, L. *Macromolecules* **2000**, *33*, 1134–1140.
- (16) Boero, M.; Parrinello, M.; Hüfner, S.; Weiss, H. *J. Am. Chem. Soc.* **2000**, *122*, 501–509.
- (17) Martinsky, C.; Minot, C.; Ricart, J. M. *Surf. Sci.* **2001**, *490*, 237–250.
- (18) Seth, M.; Margl, P.; Ziegler, T. *Macromolecules* **2002**, *35*, 7815–7829.
- (19) Vanka, K.; Xu, Z.; Seth, M.; Ziegler, T. *Top. Catal.* **2005**, *34*, 143–164.
- (20) Busico, B.; Causa, M.; Cipullo, R.; Credendino, R.; Cutillo, F.; Friederichs, N.; Lamanna, R.; Segre, A.; Castelli, V. V. A. *J. Phys. Chem. C* **2008**, *112*, 1081–1089.
- (21) Stukalov, D. V.; Zakharov, V. A. *J. Phys. Chem. C* **2009**, *113*, 21376–21382.
- (22) Bahri-Laleh, N.; Correa, A.; Mehdipour-Ataei, S.; Arabi, H.; Haghighi, M. N.; Zohuri, G.; Cavallo, L. *Macromolecules* **2011**, *44*, 778–783.
- (23) Di Noto, V.; Marigo, A.; Viviani, M.; Marega, C.; Bresadola, S.; Zannetti, R. *Makromol. Chem.* **1992**, *193*, 123–131.
- (24) Forte, M. C.; Coutinho, F. M. B. *Eur. Polym. J.* **1996**, *32*, 223–231.
- (25) Sozzani, P.; Bracco, S.; Comotti, A.; Simonutti, R.; Camurati, I. *J. Am. Chem. Soc.* **2003**, *125*, 12881–12893.
- (26) Malizia, F.; Fait, A.; Cruciani, G. *Chem.—Eur. J.* **2011**, *17*, 13892–13897.
- (27) Kim, I.; Kim, J. H.; Choi, H. K.; Chung, M. C.; Woo, S. I. *J. Appl. Polym. Sci.* **1993**, *48*, 721–730.
- (28) Czala, K.; Bialek, M. *Polymer* **2001**, *42*, 2289–2297.
- (29) Sobata, P. *Coord. Chem. Rev.* **2004**, *248*, 1047–1060.
- (30) Seenivasan, K.; Sommazzi, A.; Bonino, F.; Bordiga, S.; Groppo, E. *Chem.—Eur. J.* **2011**, *17*, 8648–8656.
- (31) Borkowsky, S. L.; Baezinger, N. C.; Jordan, R. F. *Organometallics* **1993**, *12*, 489–495.
- (32) Plecnik, C. E.; Liu, F.-C.; Liu, S.; Liu, J.; Meyers, E. A.; Shore, S. G. *Organometallics* **2001**, *20*, 3599–3606.
- (33) Kresse, G.; Furthmüller, J. *Phys. Rev. B* **1996**, *54*, 11169–11186.
- (34) Kresse, G.; Joubert, D. *Phys. Rev. B* **1999**, *59*, 1758–1775.
- (35) Grimme, S. *J. Comput. Chem.* **2006**, *27*, 1787–1799.
- (36) Frisch, M. J.; Trucks, G. W.; Schlegel, H. B.; Scuseria, G. E.; Robb, M. A.; Cheeseman, J. R.; Scalmani, G.; Barone, V.; Mennucci, B.; Petersson, G. A.; Nakatsuji, H.; Caricato, M.; Li, X.; Hratchian, H. P.; Izmaylov, A. F.; Bloino, J.; Zheng, G.; Sonnenberg, L.; Hada, M.; Ehara, M.; Toyota, K.; Fukuda, R.; Hasegawa, J.; Ishida, M.; Nakajima, T.; Honda, Y.; Kitao, O.; Nakai, H.; Vreven, T.; Montgomery, J. A., Jr.; Peralta, J. E.; Ogliaro, F.; Bearpark, M.; Heyd, J. J.; Brothers, E.; Kudin, K. N.; Staroverov, V. N.; Kobayashi, R.; Normand, J.; Raghavachari, K.; Rendell, A.; Burant, J. C.; Iyengar, S. S.; Tomasi, J.; Cossi, M.; Rega, N.; Millam, J. M.; Klene, M.; Knox, J. E.; Cross, J. B.; Bakken, V.; Adamo, C.; Jaramillo, J.; Gomperts, R.; Stratmann, R. E.; Yazyev, O.; Austin, A. J.; Cammi, R.; Pomelli, C.; Ochterski, J. W.; Martin, R. L.; Morokuma, K.; Zakrzewski, V. G.; Voth, G. A.; Salvador, P.; Dannenberg, J. J.; Dapprich, S.; Daniels, A. D.; Farkas, O.; Foresman, J. B.; Ortiz, J. V.; Cioslowski, J.; Fox, D. J. *Gaussian 09*, Revision A.02; Gaussian Inc.: Wallingford, CT, 2009.
- (37) Negishi, E. *Dalton. Trans.* **2005**, 827–848.
- (38) Wang, C.; Zhenfeng, X. *Chem Soc. Rev.* **2007**, *36*, 1395–1406.